NIH Public Access
Author Manuscript
J Cardiovasc Transl Res. Author manuscript; available in PMC 2015 March 01.

Published in final edited form as:
J Cardiovasc Transl Res. 2014 March ; 7(2): 192–202. doi:10.1007/s12265-013-9538-0.

Sex differences in translocator protein 18 kDa (TSPO) in the heart: implications for imaging myocardial inflammation

DeLisa Fairweather[1,*,†], **Michael J. Coronado**[1,*], **Amanda E. Garton**[1], **Jennifer L. Dziedzic**[2], **Adriana Bucek**[1], **Leslie T. Cooper Jr.**[3], **Jessica E. Brandt**[1], **Fatima S. Alikhan**[2], **Haofan Wang**[4], **Christopher J. Endres**[4], **Judy Choi**[2], **Martin G. Pomper**[4], and **Tomás R. Guilarte**[2,†]

[1]Johns Hopkins Bloomberg School of Public Health, 615 N. Wolfe Street, Baltimore, MD 21205, USA;

[2]Mailman School of Public Health, Columbia University, 722 W. 168th Street, New York, NY 10032, USA;

[3]Mayo Clinic 200 First Street SW, Rochester, MN 55905, USA;

[4]Johns Hopkins School of Medicine, 628 Rutland Avenue, Baltimore, MD 21205, USA.

Abstract

Myocarditis is more severe in men than women and difficult to diagnose due to a lack of imaging modalities that directly detect myocardial inflammation. Translocator protein 18 kDa (TSPO) is used extensively to image brain inflammation due to its presence in $CD11b^+$ brain microglia. In this study we examined expression of TSPO and CD11b in mice with coxsackievirus B3 (CVB3) myocarditis and biopsy sections from myocarditis patients in order to determine if it could be used to image myocarditis. We found that male mice with CVB3 myocarditis upregulated more genes associated with TSPO activation than females. TSPO expression was increased in the heart of male mice and men with myocarditis compared to females due to testosterone, where it was expressed predominantly in $CD11b^+$ immune cells. We show that TSPO ligands detect myocardial inflammation using microSPECT, with increased uptake of [^{125}I]-IodoDPA-713 in male mice with CVB3 myocarditis compared to undiseased controls.

Keywords

myocarditis; sex differences; imaging; single-photon emission computed tomography; TSPO; CD11b

Correspondence to Dr. DeLisa Fairweather, PhD, Department of Environmental Health Sciences, Johns Hopkins University Bloomberg School of Public Health, 615 N Wolfe St, Rm E7628, Baltimore, MD 21205. Ph: +1 410 955-4712, Fax: +1 410 955-0116, dfairwea@jhsph.edu. Correspondence to Dr. Tomás R. Guilarte, PhD, Department of Environmental Health Sciences, Mailman School of Public Health, Columbia University, 722 W 168th St, Rm 1105-E, New York, NY 10032. Ph: +1 212 305 3959, Fax: +1 212 305-3587, trguilarte@columbia.edu.
*Both are first authors
†Both are corresponding authors

Ethical Standard
Authors declare that the experiments in this manuscript comply with the current laws of the United States.

Conflict of Interest
The authors declare that they have no financial relationship with the funding organizations that sponsored the research. Authors have full control of the primary data and agree to allow the Journal to review the data if requested.

NIH-PA Author Manuscript
NIH-PA Author Manuscript
NIH-PA Author Manuscript

NIH-PA Author Manuscript

NIH-PA Author Manuscript

NIH-PA Author Manuscript

Introduction

Myocarditis, or inflammation of the myocardium, leads to a significant minority of dilated cardiomyopathy (DCM) cases in the United States [1]. However, the true incidence and prevalence of myocarditis are unknown due to the lack of biomarkers and imaging modalities that directly detect myocardial inflammation [1, 2]. Echocardiography and cardiac magnetic resonance imaging (cMRI) are currently used to diagnose myocarditis and measure changes in heart function, edema, fibrosis and dilation but these methods do not directly detect myocardial inflammation [3, 4]. Thus, there is a need for a non-invasive method to determine the presence and severity of myocarditis in addition to echocardiography and cMRI that does not require endomyocardial biopsy.

Translocator protein 18 kDa (TSPO), previously called peripheral benzodiazepine receptor [5], is used extensively to image brain inflammation in patients due to its presence in $CD11b^+$ brain microglia (macrophages) [6-8]. In healthy humans and rodents, the highest density of TSPO expression is found in steroidogenic tissues like the testes and ovaries, with relatively high levels also detected in the heart, lung and liver [9-11]. TSPO is the rate-limiting step in the transport of cholesterol into the inner mitochondrial membrane where it is used to make steroids [9, 10, 12, 13], and TSPO is required for expression of estrogen, progesterone and testosterone in the heart and by immune cells like macrophages [6, 9, 14, 15]. Although TSPO imaging is routinely used to assess brain inflammation in patients via positron emission tomography (PET) or single-photon emission computed tomography (SPECT) [6-8, 16, 17], and more recently to detect inflammation in atherosclerotic plaques [15, 18-20], its potential as an imaging tool for myocardial inflammation has not been previously examined.

Similar to other cardiovascular diseases, the incidence and severity of myocarditis, DCM and heart failure are higher in men and male mice with a better long-term outcome in females [21-23]. A recent clinical study of myocarditis and acute DCM patients found that myocardial recovery and transplant-free survival were significantly worse in men compared to women, driven by a marked difference in survival [23]. While most cases of suspected myocarditis are not linked to a specific cause, viral infections such as coxsackievirus B3 (CVB3) are the most commonly identified cause of myocarditis in developed countries [1, 4]. Previously we showed in a mouse model of CVB3 myocarditis that testosterone increases CD11b expression on cardiac macrophages during acute myocarditis in males [24, 25]. CD11b is also known as complement receptor 3 and is upregulated on activated macrophages/ microglia. $CD11b^+$ immune cells make up around 80% of the inflammatory infiltrate during acute CVB3 myocarditis [24], which suggests that a marker like TSPO that could detect these cells would provide information on the severity of myocarditis. Additionally, cardiac $CD11b^+$ immune cells were associated with progression from CVB3 myocarditis to DCM and heart failure in male mice [13, 21, 24, 25]. Based on these data, we hypothesized that TSPO may be present in cardiac $CD11b^+$ immune cells during myocarditis making TSPO a good candidate for imaging myocardial inflammation.

Methods

Myocarditis Patients

Myocardial inflammation was confirmed histologically in endomyocardial heart biopsies from 20 myocarditis patients at Mayo Clinic (n=10/sex). Approval was obtained from the Institutional Review Boards at the Mayo Clinic and Johns Hopkins University for the study. Procedures are in accordance with the ethical standards of the Helsinki Declaration of 1975, as revised in 2000. Some of the samples were obtained from a clinical trial that is registered

NIH-PA Author Manuscript

NIH-PA Author Manuscript

NIH-PA Author Manuscript

at www.clinicaltrials.gov (NCT0004482). All clinical samples used in this study were from patients where consent was obtained for future research.

Immunohistochemistry

Biopsy sections from myocarditis patients were de-paraffinized, blocked, stained with rabbit anti-human CD11b (Clone EP1345Y, Abcam, Cambridge, MA) at 1:250 dilution for 1h at room temperature followed by a biotinylated secondary antibody for 1h and incubated with 3,3′-diaminobenzidine (DAB) (dark brown). Tissue sections were counterstained with hematoxylin (blue background).

Animal Model

Male and female 6-8 week old BALB/cJ mice (Cat. No. 000651) were obtained from the Jackson Laboratory (Bar Harbor, ME). Mice were maintained under pathogen-free conditions in the animal facility at the Johns Hopkins School of Medicine, and approval was obtained from the Animal Care and Use Committee of Johns Hopkins University and Columbia University for all procedures. Procedures are in accordance with the ethical standards of the Helsinki Declaration of 1975, as revised in 2000. 7-10 mice/group were inoculated intraperitoneally with 10^3 plaque forming units of a heart-passaged stock of CVB3 or sterile phosphate buffered saline (PBS) and hearts and sera collected on day 10 post infection (pi), according to [26, 27]. All mouse studies conducted in this study were analyzed during peak myocarditis at day 10 pi.

Histology

Formalin-fixed hearts from myocarditis patients or mice were stained with hematoxylin and eosin to detect inflammation. Myocarditis in mice was assessed as the percentage of the heart section with inflammation compared to the overall size of the heart section using a microscope eye-piece grid, as previously [21, 24, 25].

Gonadectomy

Pre-pubertal 6 week old male BALB/c mice were bilaterally gonadectomized or received a sham operation under ketamine (50mg/kg)/ xylazine (5mg/kg) anesthesia (Phoenix Pharmaceutical, St. Joseph, MO), as previously [21, 25]. For testosterone (Te) replacement, slow-release testosterone or control pellets were implanted subcutaneously, according to [28]. Mice were allowed two weeks to recover from the operation before myocarditis was induced. Testosterone was measured in sera using a Quantikine ELISA kit (R&D Systems, Minneapolis, MN).

Microarray

Whole hearts from male and female BALB/c mice with CVB3 myocarditis were compared to normal hearts from PBS-inoculated control male and female mice by microarray (n=3/ group based on echocardiography of representative disease between sexes [21]. RNA (100ng) was processed for hybridization to Affymetrix Mouse Gene ST 1.0 microarrays using the Affymetrix GeneChip Whole Transcript Sense Target Labeling Assay (Affymetrix, Santa Clara, CA), as previously [13, 21]. The microarray was performed by the Johns Hopkins Bloomberg School of Public Health Genomic Analysis and Sequencing Core Facility. Analysis of microarray data was performed with Partek Genomics Suite (GS) Version 6.4 (Partek, MO, USA). Gene expression patterns for each gene were normalized to the median array intensity for all chips and data from infected animals were normalized to uninfected PBS controls [13, 21]. Microarray data were analyzed with Partek GS software by 2-way ANOVA in order to look for significant differences between conditions, with sex (male/ female) and treatment (PBS/ myocarditis) as factors and then P values and fold

NIH-PA Author Manuscript

NIH-PA Author Manuscript

NIH-PA Author Manuscript

changes were generated using Fisher's least significant difference (LSD) post hoc analysis for comparisons of sex. False discovery rate (FDR) corrections for multiple comparisons (Benjamini-Hochberg) were applied to reduce the total number of false-positives. Genes were considered significant if they had a P value less than 0.05. The Affymetrix gene expression data were deposited to the Gene Expression Omnibus (www.ncbi.nlm.nih.gov/geo) under Accession Number GSE35182.

qRT-PCR

Mouse hearts were perfused and digested with collagenase II (10,000 U/mL, Worthington, CLS-2) to release immune cells using a gentleMACs Dissociator. Immune cells were isolated using MACs magnetic microbeads for CD11b or CD45 (Miltenyi Biotec, Auburn, CA). Trizol Reagent and the PureLink Micro-to-Midi system (Invitrogen, Carlsbad, CA) were used for purification of RNA from total hearts or immune cells. Human RNA was isolated from heart biopsies of formalin-fixed, paraffin-embedded (FFPE) blocks from patients with histology-verified myocarditis. Human RNA was processed using a PureLink FFPE RNA Isolation Kit (Invitrogen, Carlsbad, CA). Quantitative RT-PCR (qRT-PCR) of gene expression was measured using Assay-on-Demand probe sets (Applied Biosystems, Foster City, CA) or RT^2qPCR Primer Assay (Qiagen, Venlo, Netherlands) and reactions analyzed using the ABI 7000 Taqman system, as previously [13, 21]. Hypoxanthine phosphoribosyltransferase (Hprt) was used for normalization.

Autoradiography

[^{125}I]-IodoDPA-713, used to assess TSPO levels in the heart, was synthesized using a two-step reaction process, as previously [29]. Desmethyl DPA-713 was first iodinated with [^{125}I]NaI in the presence of iodogen. The ^{125}I radiolabeled intermediate was methylated by MeI/K_2CO_3/DMF and HPLC purified. The overall radioactive yield was 35-50% with >99% radiochemical purity. Fresh-frozen hearts were sectioned (20μm) on a cryostat in the sagittal plane and thaw-mounted onto poly-L-lysine-coated slides and stored at −20°C. Slides were dried for 30min and prewashed with 50mM Tris-HCl buffer (pH 7.4). To determine total binding, slides were incubated for 1h at RT in buffer containing 0.8nM [^{125}I]-IodoDPA-713 (specific activity 2200 Ci/mmol). To measure non-specific binding, adjacent slides were incubated in the presence of 50μM cold racemic PK11195 (Sigma, St. Louis, MO). After incubation, slides were washed and exposed to film at RT for 20min. Images were captured and analyzed using MCID (InterFocus Imaging Ltd., Cambridge, England) calibrating for density using [^{125}I]-microscales. The mean value for all sections/heart was used for statistical analyses.

Saturation Isotherms (B_{max} and K_d)

Whole hearts were homogenized in 50 volumes Tris-HCl buffer (pH 7.4) and centrifuged at 40,000*g* for 30min at 4°C. The pellet was resuspended in 50 volumes of Tris-HCl buffer (pH 7.4) and recentrifuged. The pellet was resuspended in 4.5mL buffer and the protein concentration determined by Lowry Assay (BioRad Laboratories, Hercules, CA), using bovine serum albumin as a standard. The preparation was used immediately for saturation isotherms. 50μL of heart protein was incubated in a total volume of 500μL with 100μL of [^{3}H]-R-PK11195 at 4°C for 1h. Nonspecific binding was measured by incubating 50μL heart protein with 50μM cold racemic PK11195. For [^{3}H]-R-PK11195 saturation isotherms, heart protein was incubated with ligand ranging in concentration from 0.25nM to 20nM. A BRANDEL filtering system with Whatman GF/B filter paper (Brandel Ince, Gaithersburg, MD) was used to terminate the reaction. Filters were washed four times with 5mL cold 50mM Tris-HCl buffer (pH 7.4). Radioactivity trapped on the filters was measured by liquid scintillation spectrometry. The EBDA/Ligand in Kell version 6 program (Biosoft,

NIH-PA Author Manuscript

NIH-PA Author Manuscript

NIH-PA Author Manuscript

Cambridge, UK) was used to determine the maximal number of binding sites (B_{max}) and the affinity constant (K_d) using a one site model.

MicroSPECT Imaging

A micro single-photon emission computed tomography (microSPECT) small animal SPECT/ computed tomography (CT) system (Gamma Medica-Ideas) was used for image acquisition, as previously [29, 30]. Mice were anesthetized with isoflourane prior to imaging. 1-2 mCi of [^{125}I]-IodoDPA-713 was injected iv and images acquired immediately after injection. The SPECT projection data were acquired using two low energy, high resolution parallel-hole collimators with a radius of rotation of 4.65cm. The tomographic data were acquired in 512 projections to allow anatomic co-registration. Data were reconstructed using the ordered subsets-expectation maximization algorithm and analyzed using AMIDE software (SourceForge). Data were analyzed using Analysis software and a time-activity curve of [^{125}I]-IodoDPA-713 uptake determined for each mouse.

Statistical Analysis

Normally distributed data comparing two groups were analyzed using a two-tailed Student's *t* test. Nonparametric data comparing two groups were analyzed using the Mann-Whitney rank sum test with a Bonferroni correction for multiple comparisons. Analysis of microarray data was performed with Partek Genomics Suite version 6.4 (St. Louis, MO) by 2-way ANOVA to examine significant differences between conditions (with sex and myocarditis as factors). Data are expressed as mean ±standard error of the mean (SEM). *P* values less that 0.05 were considered statistically significant.

Results

TSPO Expression Detected in the Heart by Microarray

Although TSPO is known to be expressed in cardiac tissues, atherosclerotic plaques and in CD11b$^+$ microglia/ macrophages [6, 9, 15, 18-20], the relationship between TSPO and myocardial inflammation has not been previously investigated. Currently, there is a lack of noninvasive imaging modalities to directly image myocardial inflammation in patients [31]. Recently cardiac MRI was used to image myocardial inflammation in a mouse model of autoimmune myocarditis [32]. Here we chose to investigate TSPO because it regulates steroid expression in CD11b$^+$ immune cells, which comprise approximately 80% of the infiltrate and predict the severity of acute myocarditis and progression to DCM and heart failure in male mice with CVB3 myocarditis [13, 21, 24, 25].

In this study we assessed the relative expression of TSPO in the heart using microarray analysis of undiseased, PBS inoculated males and females vs. mice with CVB3 myocarditis (Table 1 and 2). We found that TSPO was significantly increased in the heart of male mice with CVB3 myocarditis compared to PBS controls by microarray (fold change 1.9, p=0.002, Table 2), but not significantly changed in females with CVB3 myocarditis (fold change 1.4, p=0.05). Twice as many genes linked to TSPO activation in macrophages, such as steroidogenic acute regulatory protein (Star) and ATP-binding cassette (Abcg1), were elevated in the heart of males with CVB3 myocarditis (25 genes) (Fig. 1A, Table 2) compared to females with myocarditis (12 genes) (Table 1) according to microarray analysis. Figure 1A illustrates genes related to TSPO that are upregulated in males during myocarditis that are important in the function of CD11b$^+$ macrophages (these genes are associated with the formation of foam cells in atherosclerosis, for example [33]. Increased expression of TSPO (p=0.0001), CD11b (p=0.0001), Star (p=0.0002), and Abcg1 (p=6x10^{-5}) was confirmed in the heart of males during CVB3 myocarditis by qRT-PCR (Fig. 1B).

NIH-PA Author Manuscript

NIH-PA Author Manuscript

NIH-PA Author Manuscript

Imaging Myocardial TSPO

PET/CT and SPECT/CT are routinely used to assess brain inflammation clinically in adults and children using TSPO-specific ligands like PK11195 and DPA-713 [6, 11, 34, 35]. These imaging modalities have been miniaturized for use in small animals (i.e. microSPECT) and have been found to be an increasingly useful tool for translating human studies [36]. Next we asked whether TSPO imaging could be used to detect myocardial inflammation in mice. We used *in vivo* [^{125}I]-IodoDPA-713 microSPECT to assess TSPO expression in the heart during acute CVB3 myocarditis in male BALB/c mice. MicroSPECT/CT imaging revealed higher TSPO radioligand uptake in the heart during CVB3 myocarditis compared to PBS inoculated controls (Fig. 2A), that was verified by quantitative analysis (n=3/group, p=0.01) (Fig. 2B). TSPO uptake in the lung (red lobes around the heart) (Fig. 2A) was not significantly different during CVB3 myocarditis than PBS controls (n=3/group, p=0.83), demonstrating that TSPO uptake could be detected at higher levels in hearts with myocarditis compared to healthy controls (Fig. 2B).

Sex Differences in Cardiac TSPO Expression

Although most inflammatory brain diseases occur more frequently and are more severe in men than women [37], to our knowledge there are no published reports of sex differences in TSPO expression in brain microglia. Because TSPO is necessary for steroid synthesis within immune and cardiac cells, we investigated whether sex differences existed in TSPO expression in the heart using quantitative receptor autoradiography of [^{125}I]-IodoDPA-713 binding, saturation isotherms and Scatchard analysis of [^{3}H]-R-PK11195 binding, and qRT-PCR [6, 29]. Traditionally, TSPO is characterized in animal models using radioligand binding assays and autoradiography due to the lack of suitable TSPO-reactive antibodies for flow cytometry or ELISA and because TSPO deficiency in mice is embryonically lethal, while conditional knockouts are not yet available [6, 38]. We found that PBS-treated females had higher constitutive TSPO binding (proportional p=0.005, density p=0.02) and mRNA levels (p=0.02) than PBS-treated males (Fig. 3A-D). TSPO levels were significantly increased in males with acute CVB3 myocarditis compared to control males by qRT-PCR (Fig. 1B) and by proportional area (p=0.03) or total density (p=0.04) of [^{125}I]-IodoDPA-713 radioligand binding (Fig. 3B,C), but not for females with myocarditis compared to PBS controls (p=0.3) (Fig. 3B) confirming the microarray data (Table 1 and 2). The binding affinity (K_d) of [^{3}H]-R-PK11195 for TSPO did not differ significantly between controls or CVB3 myocarditis in males or females (PBS vs. CVB3 females p=0.40, PBS vs. CVB3 males p=0.39, PBS males vs. females p=0.07, Bonferroni correction p=0.29; CVB3 males vs. females p=0.33) (Fig. 4B, left). However, TSPO levels were increased in males and females with CVB3 myocarditis compared to controls when assessing the maximum number of [^{3}H]-R-PK11195 binding sites (B_{max}) (PBS vs. CVB3 females p=0.002, Bonferroni correction p=0.009; PBS vs. CVB3 males p=0.01, Bonferroni correction p=0.04) (Fig. 4B, right).

To determine whether sex differences existed in cardiac TSPO expression in myocarditis patients, we extracted RNA from myocardial biopsy samples with histology-verified myocarditis and examined TSPO mRNA levels by qRT-PCR. We found that men with myocarditis had significantly higher expression of TSPO in the heart than women (n=10/sex, p=0.03) (Fig. 3E). Overall, these data indicate that sex differences in TSPO expression exist in the heart during CVB3 myocarditis.

TSPO Expression in Cardiac CD11b^{+} Immune Cells

TSPO is expressed during brain inflammation within CD11b^{+} microglia/ macrophages [6-8]. CD11b, also known as complement receptor 3, is upregulated on activated immune cells like macrophages following infection [24]. We showed previously using flow cytometry that

NIH-PA Author Manuscript

NIH-PA Author Manuscript

NIH-PA Author Manuscript

male mice with CVB3 myocarditis have more $CD11b^+$ immune cells in the heart than females [24] that is due to testosterone [25]. Here we found that CD11b mRNA expression was significantly higher in the heart of male mice with CVB3 myocarditis compared to females (n=10/sex, p=0.02) (Fig. 3F) and in men with histology-proven myocarditis compared to women (n=7/sex, p=0.003) (Fig. 3G). Typical $CD11b^+$ staining by immunohistochemistry is shown from a myocarditis patient (Fig. 5, right) indicating that, similar to CVB3 myocarditis [24, 25], most of the inflammatory cells in the heart of myocarditis patients express CD11b. To determine whether TSPO was present in $CD11b^+$ immune cells during CVB3 myocarditis in mice, we separated $CD11b^+$ cells from other immune cells using magnetic beads and examined TSPO levels by qRT-PCR. We found that TSPO was expressed predominantly in $CD11b^+$ inflammatory cells compared to other immune cell types during CVB3 myocarditis (n=9/group, p=0.04) (Fig. 3H), similar to findings with brain inflammation. These data suggest that TSPO would be a good biomarker to assess the severity of myocarditis.

Testosterone Increases TSPO Expression in Immune Cells

To determine whether testosterone was responsible for sex differences in TSPO levels in the heart during CVB3 myocarditis, we gonadectomized (Gdx) or removed the testes from male BALB/c mice or performed a sham operation (to control for the stress of the operation which affects the inflammatory response) and inserted a control (Con) or slow-release testosterone (Te) pellet subcutaneously (which should reverse the effect of Gdx if testosterone is responsible for the effect), as previously [21, 25]. After recovery all mice were infected with CVB3 to induce myocarditis and TSPO levels assessed at day 10 pi during the peak of acute myocarditis. We found that removing the testes in Gdx-Con mice significantly decreased myocarditis (Fig. 6A,B), circulating Te levels (Fig. 6C), and TSPO mRNA levels in the whole heart by qRT-PCR (Fig. 6D) compared to Sham-Con mice, indicating that testosterone increases TSPO levels in the heart. Testosterone replacement in Gdx males (Gdx-Te) restored myocarditis (Fig. 6A,B) and circulating Te levels (Fig. 6C) confirming that testosterone was responsible for the decreased myocarditis in Gdx mice. However, testosterone replacement in Gdx males (Gdx-Te) did not increase TSPO mRNA levels from whole hearts (which is composed primarily of cardiac myocytes, fibroblasts and immune cells), which remained low like the Gdx-Con group (Fig. 6D). This finding suggests that testosterone was not increasing TSPO levels in cardiac tissues in general. Because sex differences in TSPO expression in the heart appeared to be due to greater TSPO expression in immune cells in males (Fig. 3H), we performed Gdx and Te replacement and isolated $CD45^+$ immune cells using magnetic beads (CD45 is a general marker for immune cells). We found that Gdx significantly lowered TSPO levels in $CD45^+$ immune cells in the heart that was reversed with Te replacement (Fig. 6E). Thus, these data show that testosterone specifically increases $TSPO^+$ immune cells in the heart during CVB3 myocarditis in male mice.

Discussion and Translational Relevance

In this preclinical study we demonstrate that TSPO ligands can be used to directly detect inflammation during myocarditis in mice. Because TSPO is present in the majority of inflammatory cells in the heart during myocarditis, it should also provide a good measure of the severity of disease. Although TSPO imaging is routinely used to assess brain inflammation [6-8, 17], and more recently to detect inflammation in atherosclerotic plaques [15, 18-20], we are the first to report that imaging based on TSPO ligands and SPECT/CT can be used to detect myocardial inflammation during myocarditis. Although myocarditis is diagnosed based on echocardiography, cMRI and endomyocardial biopsy [3], there are currently no noninvasive imaging tools that allow direct assessment of myocardial

NIH-PA Author Manuscript

NIH-PA Author Manuscript

NIH-PA Author Manuscript

inflammation in patients. The ability to directly image myocardial inflammation noninvasively would improve diagnosis made by echocardiography and cMRI and allow earlier detection of disease. Knowing TSPO levels may additionally predict myocarditis patients that are at an increased risk to progress to DCM and heart failure. Furthermore, imaging for myocardial inflammation could be used to assess the efficacy of therapeutic strategies. Future studies should examine the effectiveness of TSPO imaging in male and female myocarditis and DCM patients compared to healthy controls.

We are the first to report that TSPO expression is able to distinguish differences in the severity of myocarditis between males and females in mice and humans. Although most inflammatory brain diseases occur more frequently and are more severe in men than women [37], to our knowledge no one has examined whether sex differences in TSPO expression occur in brain microglia. Whether sex differences exist in TSPO levels in atherosclerotic plaques has also not been investigated. Baseline sex differences in TSPO levels in the heart were found in mice, with females having higher constitutive expression of TSPO than males prior to disease. A potential explanation for sex differences in TSPO levels is that steroid hormone response elements, including those activated by the androgen or estrogen receptor, have been identified within mouse and human *Tspo* promoters, suggesting that sex hormones influence TSPO expression [10]. Interestingly, administration of TSPO ligands have been found to alter testosterone and estrogen levels in sera [39], perhaps indicating a positive feedback loop [13]. Our finding that testosterone increased TSPO primarily in immune cells in the heart during CVB3 myocarditis suggests that the higher cardiac TSPO expression observed in men and male mice with myocarditis may be due to more $TSPO^{+}$ CD11b cells in the inflammatory infiltrate of males than females. Activation of monocytes in culture is known to upregulate TSPO expression that tracks with elevated CD11b, tumor necrosis factor, interleukin (IL)-1 and IL-8 [40, 41], suggesting a relationship between TSPO activation and immune function [13]. Interestingly, TSPO has been detected on the cell membrane of immune cells and in compartments of the cell devoid of mitochondria suggesting that TSPO has physiologic functions in immune cells besides regulating mitochondrial activity [9, 42]. We found previously that activation of the androgen receptor and TSPO in the spleen during the innate immune response to CVB3 infection are associated with inflammatory gene changes that confer susceptibility to cardiovascular disease [13]. Future studies should examine whether TSPO promotes acute inflammation that leads to more severe myocarditis and DCM in males. This preclinical study suggests that TSPO ligands can be used as a noninvasive imaging technique to detect myocardial inflammation in men and women with myocarditis and inflammatory DCM. Future studies will need to determine baseline expression levels of TSPO in the hearts of healthy men and women to determine whether levels are increased enough during cute myocarditis to be diagnostically or therapeutically useful.

Acknowledgments

Funding

This work was supported by National Institutes of Health (NIH) awards from the National Heart, Lung and Blood Institute [grant numbers HL087033, HL111938] to D.F and M.J.C., an American Heart Association Grant-in-Aid [12GRNT12050000] to D.F., and a National Institute of Environmental Health Science (NIEHS) training grant [ES07141] to M.J.C. T.R.G. is supported by a NIH award from the NIEHS [ES07062].

References

1. Cooper LT Jr. Myocarditis. N Engl J Med. 2009; 9:1526–1538. [PubMed: 19357408]
2. Schultheiss HP, Kuhl U, Cooper LT Jr. The management of myocarditis. Eur Heart J. 2011; 32:2616–2625. [PubMed: 21705357]

NIH-PA Author Manuscript

NIH-PA Author Manuscript

NIH-PA Author Manuscript

3. Friedrich MG, Sechtem U, Schulz-Menger J, Holmvang G, Alakija P, Copper LT, White JA, Abdel-Aty H, Gutberlet M, Prasad S, Aletras A, Laissy JP, Paterson I, Filipchuk NG, Kumar A, Pauschnger M, Liu P, International Consensus Group on Cardiovascular Magnetic Resonance in Myocarditis. Cardiovascular magnetic resonance in myocarditis: a JACC White Paper. J Am Coll Cardiol. 2009; 53:1475–1487. [PubMed: 19389557]
4. El Amm C, Fairweather D, Cooper LT Jr. Pathogenesis and diagnosis of myocarditis. Heart. 2012; 98:835–840. [PubMed: 22442199]
5. Papadopoulos V, Baraldi M, Guilarte TR, Knudsen TB, Lacapere JJ, Lindemann P, Norenberg MD, Nutt D, Weizman A, Zhang MR, Gavish M. Translocator protein (18kDa): new nomenclature for the peripheral-type benzodiazepine receptor based on its structure and molecular function. Trends Pharmacol Sci. 2006; 27:402–409. [PubMed: 16822554]
6. Chen MK, Guilarte TR. Translocator protein 18 kDa (TSPO): molecular sensor of brain injury and repair. Pharmacol Ther. 2008; 118:1–17. [PubMed: 18374421]
7. Rupprecht R, Papadopoulos V, Rammes G, Baghai TC, Fan J, Akula N, Groyer G, Adams D, Schumacher M. Translocator protein (18 kDa) (TSPO) as a therapeutic target for neurological and psychiatric disorders. Nat Rev Drug Discov. 2010; 9:971–988. [PubMed: 21119734]
8. Rampani A, Palazzo C, de Candia M, Lasorsa FM, Trapani G. Targeting of the translocator protein 18 kDa (TSPO): a valuable approach for nuclear and optical imaging of activated microglia. Bioconjug Chem. 2013; 24:1415–1428. [PubMed: 23837837]
9. Veenman L, Gavish M. The peripheral-type benzodiazepine receptor and the cardiovascular system. Implications for drug development. Pharmacol Ther. 2006; 110:503–524. [PubMed: 16337685]
10. Batarseh A, Papadopoulos V. Regulation of translocator protein 18kDa (TSPO) expression in health and disease states. Mol Cell Endocrinol. 2010; 327:1–12. [PubMed: 20600583]
11. Endres CJ, Coughlin JM, Gage KL, Watkins CC, Kassiou M, Pomper MG. Radiation dosimetry and biodistribution of the TSPO ligand 11C-DPA-713 in humans. J Nucl Med. 2012; 53:330–335. [PubMed: 22241913]
12. Miller WL. Steroid hormone synthesis in mitochondria. Mol Cell Endocrinol. 2013; 379:62–73. [PubMed: 23628605]
13. Onyimba JA, Coronado MJ, Garton AE, Kim JB, Bucek A, Bedja D, Gabrielson KL, Guilarte TR, Fairweather D. The innate immune response to coxsackievirus B3 predicts progression to cardiovascular disease and heart failure in male mice. Biol Sex Differ. 2011; 2:2. [PubMed: 21338512]
14. Surinkaew S, Chattipakorn S, Chattipakorn N. Roles of mitochondrial benzodiazepine receptor in the heart. Can J Cardiol. 2011; 27:262.e3–13. [PubMed: 21459278]
15. Gaemperli O, Shalhoub J, Owen DR, Lamare F, Johansson S, Fouladi N, Davies AH, Rimoldi OE, Camici PG. Imaging intraplaque inflammation in carotid atherosclerosis with 11C-PK11195 positron emission tomography/computed tomography. Eur Heart J. 2012; 33:1902–1910. [PubMed: 21933781]
16. Versijpt J, Dumont F, Thierens H, Jansen H, DeVos F, Slegers G, Santens P, Dierckx RA, Korf J. Biodistribution and dosimetry of [^{123}I]iodo-PK 11195: a potential agent for SPECT imaging of the peripheral benzodiazepine receptor. Eur J Nucl Med. 2000; 27:1326–1333. [PubMed: 11007514]
17. Debruyne JC, Versijpt J, van Laere KJ, De Vos F, Keppens J, Strijckmans K, Achten E, Slegers G, Dierckx RA, Korf J, De Reuck JL. PET visualization of microglia in multiple sclerosis patients using [^{11}C]PK11195. Eur J Neurol. 2003; 10:257–264. [PubMed: 12752399]
18. Fujimura Y, Hwang PM, Trout H III, Kozloff L, Imaizumi M, Innis RB, Fujita M. Increased peripheral benzodiazepine receptors in arterial plaque of patients with atherosclerosis: an autoradiographic study with [^{3}H]PK11195. Atherosclerosis. 2008; 201:108–111. [PubMed: 18433754]
19. Pugliese F, Gaemperli O, Kinderlerer AR, Lamare F, Ahalhoub J, Davies AH, Rimoldi OE, Mason JC, Camici PG. Imaging of vascular inflammation with [^{11}C]-PK11195 and positron emission tomography/computed tomography angiography. J Am Coll Cardiol. 2010; 56:653–661. [PubMed: 20705222]

NIH-PA Author Manuscript

NIH-PA Author Manuscript

NIH-PA Author Manuscript

20. Lamare F, Hinz R, Gaemperli O, Pugliese F, Mason JC, Spinks T, Camici PG, Rimoldi OE. Detection and quantification of large-vessel inflammation with ^{11}C-R-PK11195 PET/CT. J Nucl Med. 2011; 52:33–39. [PubMed: 21149475]
21. Coronado MJ, Brandt JE, Kim E, Bucek A, Bedja D, Abston ED, Shin J, Gabrielson KL, Mitzner W, Fairweather D. Testosterone and interleukin-1 increase cardiac remodeling during acute coxsackievirus B3 myocarditis via serpin A 3n. Am J Physiol Heart Circ Physiol. 2012; 302:H1726–H1736. [PubMed: 22328081]
22. Fairweather D, Cooper LT Jr, Blauwet LA. Sex and gender differences in myocarditis and dilated cardiomyopathy. Curr Probl Cardiol. 2013; 38:7–46. [PubMed: 23158412]
23. McNamara DM, Starling RC, Cooper LT, Boehmer JP, Mather PJ, Janosko KM, Gorcsan J 3rd, Kip KE, Dec GW, IMAC Investigators. Clinical and demographic predictors of outcomes in recent onset dilated cardiomyopathy: results of the IMAC (Intervention in Myocarditis and Acute Cardiomyopathy)-2 study. J Am Coll Cardiol. 2011; 58:1112–1118. [PubMed: 21884947]
24. Frisancho-Kiss S, Davis SE, Nyland JF, Frisancho JA, Cihakova D, Rose NR, Fairweather D. Cutting edge: cross-regulation by TLR4 and T cell Ig mucin-3 determines sex differences in inflammatory heart disease. J Immunol. 2007; 178:6710–6714. [PubMed: 17513715]
25. Frisancho-Kiss S, Coronado MJ, Frisancho JA, Lau VM, Rose NR, Klein SL, Fairweather D. Gonadectomy of male BALB/c mice increases Tim-3+ alternatively activated M2 macrophages, Tim-3+ T cells, Th2 cells and Treg in the heart during acute coxsackievirus-induced myocarditis. Brain Behav Immun. 2009; 23:649–657. [PubMed: 19126426]
26. Fairweather D, Rose NR. Coxsackievirus-induced myocarditis in mice: a model of autoimmune disease for studying immunotoxicity. Methods. 2007; 41:118–1122. [PubMed: 17161308]
27. Myers JM, Fairweather D, Huber SA, Cunningham MW. Autoimmune myocarditis, valvulitis, and cardiomyopathy. Curr Protoc Immunol Chapter 15: Unit 15. 2013; 14:1–51.
28. Klein SL, Bird BH, Glass GE. Sex differences in Seoul virus infection are not related to adult sex steroid concentrations in Norway rats. J Virol. 2000; 74:8213–8217. [PubMed: 10933735]
29. Wang H, Pullambhatla M, Guilarte TR, Mease RC, Pomper MG. Synthesis of [^{125}I]iodoDPA-713: a new probe for imaging inflammation. Biochem Biophys Res Commun. 2009; 389:80–83. [PubMed: 19703411]
30. Banerjee SR, Pullambhatia M, Byun Y, Nimmagadda S, Foss CA, Green G, Fox JJ, Lupold SE, Mease RC, Pomper MG. Sequential SPECT and optical imaging of experimental models of prostate cancer with a dual modality inhibitor of the prostate-specific membrane antigen. Angew Chem Int Ed Engl. 2011; 50:9167–9170. [PubMed: 21861274]
31. Cooper LT, Jr; Fairweather, D. We only see what we look for: imaging cardiac inflammation. Circ Cardiovasc Imaging. 2013; 6:165–166. [PubMed: 23512779]
32. Van Heeswijk RB, De Blois J, Kania G, Gonzales C, Blyszczuk P, Stuber M, Eriksson U, Schwitter J. Selective in vivo visualization of immune cell infiltration in a mouse model of autoimmune myocarditis by fluorine-19 cardiac magnetic resonance. Circ Cardiovasc Imaging. 2013; 6:277–284. [PubMed: 23343515]
33. Yuan Y, Li P, Ye J. Lipid homeostasis and the formation of macrophage-derived foam cells in atherosclerosis. Protein Cell. 2012; 3:173–181. [PubMed: 22447659]
34. Endres CJ, Pomper MG, James M, Uzuner O, Hamoud DA, Watkins CC, Reynolds A, Hilton J, Dannals RF, Kassiou M. Initial evaluation of 11C-DPA-713, a novel TSPO PET ligand, in humans. J Nucl Med. 2009; 50:1276–1282. [PubMed: 19617321]
35. Kumar A, Muzik O, Shandal V, Chugani D, Chakraborty P, Chugani HT. Evaluation of age-related changes in translocator protein (TSPO) in human brain using (11)C-[R]-PK11195 PET. J Neuroinflammation. 2012; 9:232. [PubMed: 23035793]
36. Suwijn SR, de Bruin K, de Bie RN, Booij J. The role of SPECT imaging of the dopaminergic system in translational research on Parkinson's disease. Parkinsonism Relat Disord. 2014; 20S1:S184–S186. [PubMed: 24262177]
37. Kipp M, Berger K, Clarner T, Dang J, Beyer C. Sex steroids control neuroinflammatory processes in the brain: relevance for acute ischaemia and degenerative demyelination. J Neuroendocrinol. 2012; 24:62–70. [PubMed: 21592237]

NIH-PA Author Manuscript

NIH-PA Author Manuscript

NIH-PA Author Manuscript

38. Papadopoulos V, Amri H, Boujrad N, Cascio C, Culty M, Garnier M, Hardwick M, Li H, Vidic B, Brown AS, Reversa JL, Bernassau JM, Drieu K. Peripheral benzodiazepine receptor in cholesterol transport and steroidogenesis. Steroids. 1997; 62:21–28. [PubMed: 9029710]

39. Lacapere J-J, Papadopoulos V. Peripheral-type benzodiazepine receptor: structure and function of a cholesterol-binding protein in steroid and bile acid biosynthesis. Steroids. 2003; 68:569–585. [PubMed: 12957662]

40. Canat X, Guillaumont A, Bauaboula M, Poinot-Chazel C, Drocq JM, Carayon P, LeFur G, Casellas P. Peripheral benzodiazepine receptor modulation with phagocyte differentiation. Biochem Pharmacol. 1993; 46:551–554. [PubMed: 8394087]

41. Choi J, Ifuku M, Noda M, Guilarte TR. Translocator protein (18 kDa)/ peripheral benzodiazepine receptor specific ligands induce microglia functions consistent with an activated state. Glia. 2011; 59:219–230. [PubMed: 21125642]

42. Cahard D, Canat X, Caryon P, Roque C, Casellas P, Le Fur G. Subcellular localization of peripheral benzodiazepine receptors on human leukocytes. Lab Invest. 1994; 70:23–28. [PubMed: 8302015]

NIH-PA Author Manuscript

NIH-PA Author Manuscript

NIH-PA Author Manuscript

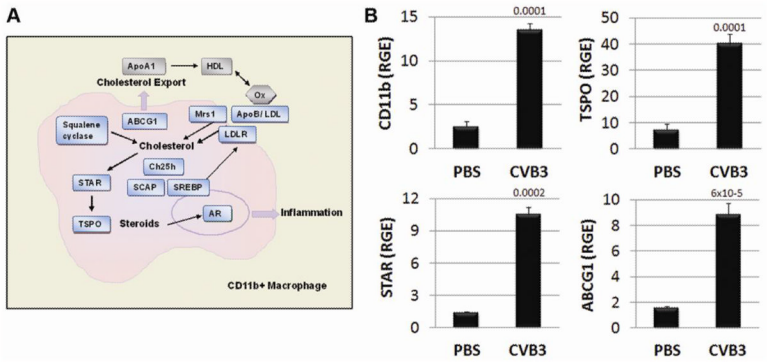

Figure 1.

TSPO-related genes upregulated in the heart of mice during CVB3 myocarditis. (**A**) Cartoon of relationship of genes related to cholesterol influx/ metabolism and TSPO-related steroid synthesis that occur in $CD11b^{+}$ immune cells like macrophages. Several of the genes found to be upregulated in the heart of males with CVB3 myocarditis at day 10 pi compared to PBS control males by microarray (see Table 2) are shown in blue. (**B**) Verification by qRT-PCR of several genes upregulated in the heart of male mice with CVB3 myocarditis compared to PBS inoculated controls. Data show the mean relative gene expression (RGE) ±SEM of 7-10 mice/group. PBS vs. CVB3 analyzed using the Mann-Whitney rank sum test.

NIH-PA Author Manuscript

NIH-PA Author Manuscript

NIH-PA Author Manuscript

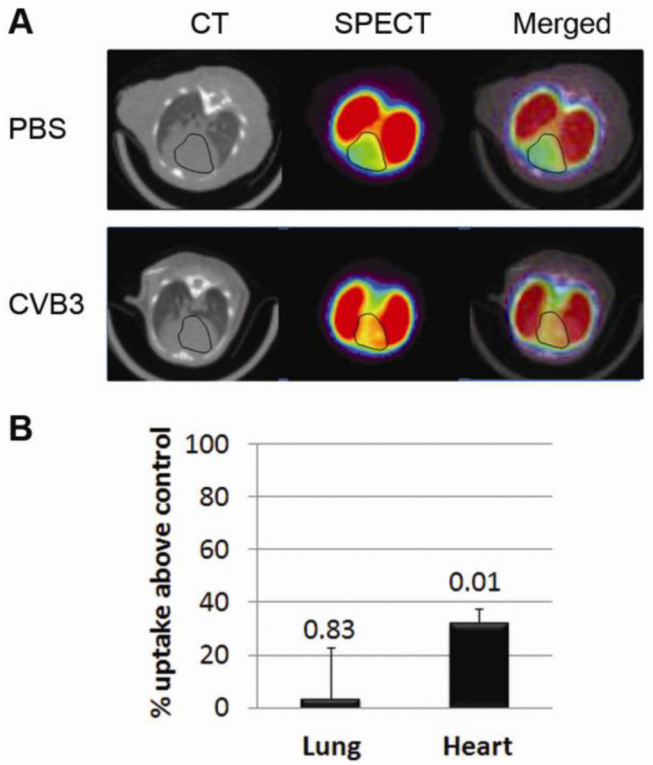

Figure 2.

MicroSPECT imaging detects myocardial inflammation in male mice with myocarditis. (**A**) Representative x-ray computed tomography (CT) and single photon emission computed tomography (SPECT) images of the lung (red lobes) and heart (outlined) from male mice inoculated either with PBS or CVB3 to induce myocarditis. [^{125}I]-IodoDPA-713 was used to image TSPO expression. (**B**) Quantitation of [^{125}I]-IodoDPA-713 binding to TSPO in the lung and heart of male mice at day 10 pi during acute CVB3 myocarditis vs. control males that received PBS. Data show the mean % uptake over controls ±SEM of 3 mice/group analyzed using paired Student's *t* test.

NIH-PA Author Manuscript
NIH-PA Author Manuscript
NIH-PA Author Manuscript

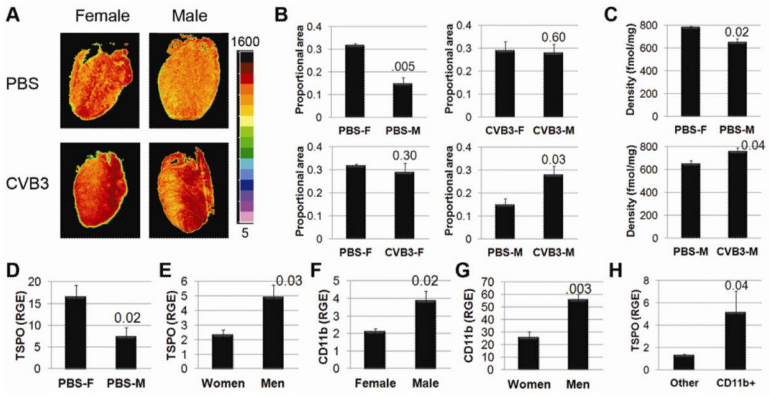

Figure 3.

TSPO and CD11b expression in the heart during myocarditis. (**A**) Representative pseudocolor images of [^{125}I]-IodoDPA-713 binding to TSPO autoradiograms in sagittal heart sections from PBS control or male and female mice with CVB3 myocarditis (day 10 pi). (**B**) Proportional area of hearts with high [^{125}I]-IodoDPA-713 TSPO-specific binding compared to the entire heart section of PBS or CVB3 inoculated male (M) and female (F) mice at day 10 pi. (**C**) Average density of [^{125}I]-IodoDPA-713 binding in heart sections at day 10 pi. (**B,C**) Data from 20 sections/heart (n = 4/group). One of three separate experiments shown that yielded the same results. (**D**) Relative gene expression (RGE) of TSPO in the heart by qRT-PCR in male and female mice inoculated with PBS (n=10/group). (**E**) TSPO expression in the heart of patients with histology-verified myocarditis using qRT-PCR (n=10/group). (**F**) CD11b expression in the heart of male and female mice with CVB3 myocarditis at day 10 pi (n=10/group). (**G**) CD11b expression in the heart of patients with histology-verified myocarditis using qRT-PCR (n=7/group). (**H**) TSPO mRNA expression in CD11b^{+} vs. other immune cells extracted from the heart using magnetic beads during CVB3 myocarditis in male mice at day 10 pi (n=9). (**B-H**) Data show the mean ±SEM analyzed by Mann-Whitney rank sum test.

NIH-PA Author Manuscript

NIH-PA Author Manuscript

NIH-PA Author Manuscript

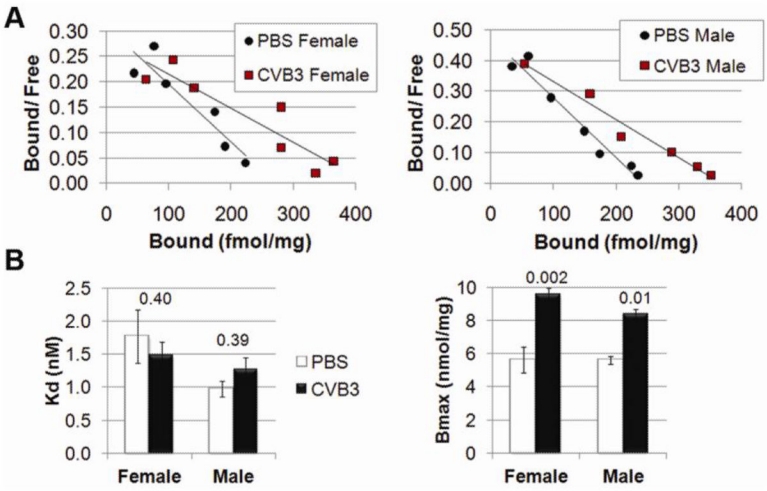

Figure 4.

Maximum number of binding sites (B_{max}) and affinity (K_d) of [^{3}H]-R-PK11195 binding to TSPO in the heart of mice. (**A**) Scatchard plots of [^{3}H]-R-PK11195 binding in the heart of female (left) and male (right) mice with CVB3 myocarditis vs. PBS controls at day 10 pi. Representative binding for individual hearts shown. (**B**) K_d (left) and B_{max} (right) for [^{3}H]-R-PK11195 binding in the heart of male and female mice with CVB3 myocarditis vs. PBS controls at day 10 pi. Data show the mean ±SEM in 3-5 hearts/group analyzed using the Mann-Whitney rank sum test (see text for *p* values after Bonferroni correction).

NIH-PA Author Manuscript
NIH-PA Author Manuscript
NIH-PA Author Manuscript

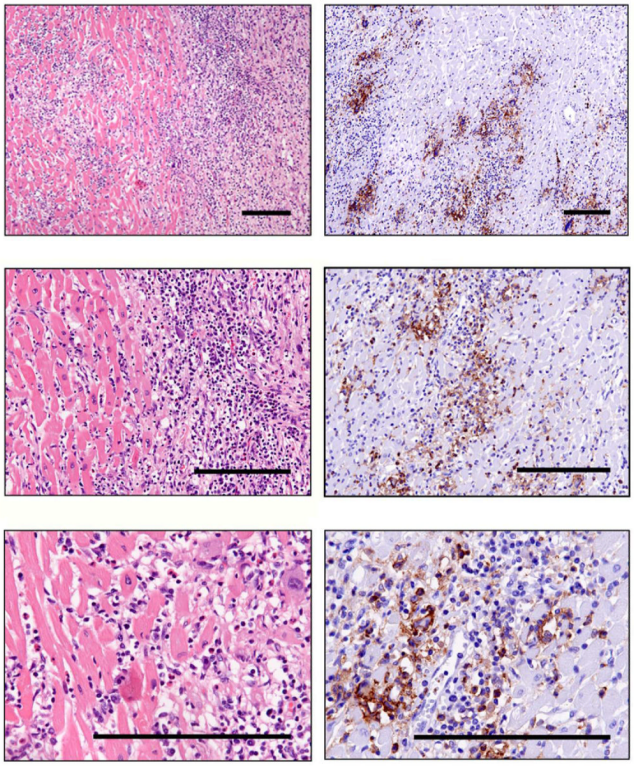

Figure 5.
CD11b expression in the heart of a myocarditis patient. Representative H&E histology sections show inflammatory cells that stain dark purple (left) or $CD11b^{+}$ immune cells that stain brown using immunohistochemistry (right) from a patient with myocarditis. Scale bar = 200μm.

NIH-PA Author Manuscript

NIH-PA Author Manuscript

NIH-PA Author Manuscript

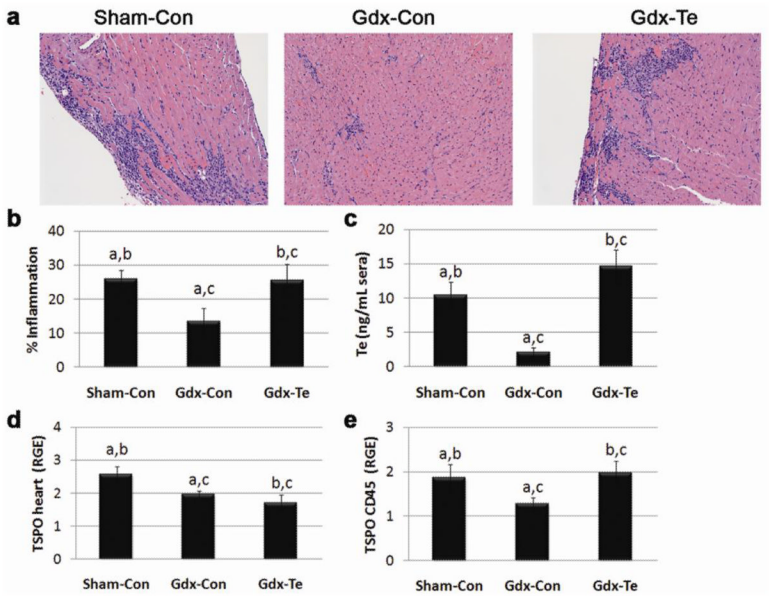

Figure 6.

Testosterone increases TSPO expression in inflammatory cells in the heart during CVB3 myocarditis at day 10 pi. (**A**) Representative H&E histology sections of CVB3 myocarditis in male mice that received a sham operation and control pellet (Sham-Con), were gonadectomized (Gdx) and received a control pellet (Gdx-Con), or were Gdx and received testosterone replacement (Gdx-Te). Magnification x64. (**B**) Myocarditis was assessed from histology sections as the percentage of the heart with inflammation compared to the overall size of the heart section using a microscope eye-piece grid (n=15-30 mice/group). Student's t test p values a=0.0003, b=0.95, c=0.02 (Bonferroni correction a=0.0001, b=1.0, c=0.06). (**C**) Serum levels of Te were measured by ELISA (n=10/group). Mann-Whitney rank sum test p values a=0.001, b=0.29, c=1.09×10^{-5} (Bonferroni correction a=0.004, b=0.87, c=3.26×10^{-5}). (**D**) Relative gene expression (RGE) of TSPO in whole hearts by qRT-PCR (n=10/group). Student's t test p values a=0.04, b=0.02, c=0.37 (Bonferroni correction a=0.12, b=0.06, c=1.0). (**E**) $CD45^+$ immune cells were isolated from the heart of males with CVB3 myocarditis using magnetic microbead isolation and RGE of TSPO assessed by qRT-PCR (n=10 mice/group). Mann-Whitney rank sum test p values a=0.06, b=0.85, c=0.01 (Bonferroni correction a=0.18, b=1.0, c=0.03).

NIH-PA Author Manuscript

NIH-PA Author Manuscript

NIH-PA Author Manuscript

Table 1

TSPO-related genes upregulated in females during CVB3 myocarditis*

GenBank	Gene	Gene name	Fold increase	*P* value
NM_013737	Pla2g7	Phospholipase A2 group VII (secreted)	2.01	0.01
NM_009593	Abcg1	ATP-binding cassette, macrophage	1.87	0.01
NM_009695	Apoc2	Apolipoprotein C-II	1.60	0.03
NM_022325	Ctsz	Cathepsin Z	1.58	0.01
NM_010299	Gm2a	GM2 ganglioside activator protein	1.46	0.03
NM_173413	Rab8b	Member RAS oncogene family	1.44	0.02
NM_023196	Pla2g12a	Phosphlipase A2 group XIIa (secreted)	1.40	0.02
NM_023409	Npc2	Niemann-Pick type C2	1.37	0.04
NM_0101422	Hexb	Hexoaminidase B	1.36	0.03
NM_023126	Rab8a	Member RAS oncogene family	1.34	0.007
NM_134154	Slc25a45	ANT 1, solute carrier family 25	1.21	0.02
NM_007824	Cyp7a1	Cytochrome P450, family 7, subfamily a	1.15	0.008

* Gene differences in the heart compare PBS inoculated to female mice with acute CVB3 myocarditis

NIH-PA Author Manuscript

NIH-PA Author Manuscript

NIH-PA Author Manuscript

Table 2

TSPO-related genes upregulated in males with CVB3 myocarditis*

GenBank	Gene	Gene name	Fold increase	*P* value
NM_001134391	Apobec1	Apolipoprotein B mRNA editing enzyme	3.51	0.001
NM_009890	Ch25h	Cholesterol 25-hydroxylase	2.82	0.02
NM_007470	Apod	Apolipoprotein D	2.29	0.007
NM_009593	Abcg1	ATP-binding cassette, macrophage	2.11	0.007
NM_009775	Tspo	Translocator protein 18kDa	1.90	0.002
NM_027976	Acsl5	Acyl CoA synthetase long-chain family	1.87	0.0004
NM_011485	Star	Steriodogenic acute regulatory protein	1.71	0.002
NM_023409	Npc2	Niemann-Pick type C2	1.70	0.002
NM_001033600	Acsl4	Acyl CoA synthetase long-chain family	1.55	0.0009
NM_023126	Rab8a	Member RAS oncogene family 8a	1.52	0.001
NM_173413	Rab8b	Member RAS oncogene family 8b	1.50	0.01
NM_009696	Apoe	Apolipoprotein E	1.45	0.001
NM_133706	Tmem97	Transmembrane protein 97	1.43	0.0003
NM_010700	Ldlr	LDL receptor	1.40	0.003
NM_146006	Lss	Lanosterol synthase (squalene cyclase)	1.40	0.002
NM_137006	Tmem97	Transmembrane protein 97	1.36	0.02
NM_013492	Clu	Clusterin (ApoJ)	1.33	0.006
NM_028766	Tmem43	Transmembrane protein 43	1.30	0.02
NM_013454	Abca1	ATP-binding cassette, sub-family A	1.29	0.02
NM_022816	Acot10	Acyl CoA thioesterase 10	1.29	0.04
NM_001177730	Nr1h3	Liver X receptor (LXR) alpha	1.26	0.03
NM_013672	Sreb1	Sterol regulatory binding TF	1.23	0.005
NM_134154	Slc25a45	ANT1, solute carrier family 25	1.22	0.01
NM_021547	Stard3	StAR-related lipid transfer domain	1.19	0.04
NM_001001144	Scap	SREBF chaperon	1.18	0.01

*Gene differences in the heart compare PBS inoculated to male mice with CVB3 myocarditis